

Article

Integrated Inundation Modeling of Flooded Water in Coastal Cities

Eun Taek Shin ¹, Jaehyun Shin ², Dong Sop Rhee ³, Hyung-Jun Kim ³ and Chang Geun Song ^{1,*}

¹ Department of Safety Engineering, Incheon National University, Incheon 22012, Korea; euntaek.shin@outlook.com

² Department of Civil & Environmental Engineering, Seoul National University, Seoul 08826, Korea; mypath@snu.ac.kr

³ Multi Disaster Countermeasure Organization, Korea Institute of Civil Engineering and Building Technology, Gyeonggi-do 10223, Korea; dsrhee@kict.re.kr (D.S.R.); john0705@kict.re.kr (H.-J.K.)

* Correspondence: baybreeze119@inu.ac.kr; Tel.: +82-032-835-8291

Received: 15 February 2019; Accepted: 27 March 2019; Published: 29 March 2019



Abstract: Climate change has increased the damage caused by subtropical rainfall and typhoons in coastal areas. Major flooding factors in coastal areas can be classified as storm surges, river inundation, and inland submergence. Because previous studies usually applied a linear sum of individual inundation components to predict comprehensive flood phenomena, this approach does not consider weighted effects associated with the simultaneous occurrence of complex flooding. In this study, a series of comprehensive flood simulations were performed using two numerical models: HDM-2D and FLUval Modeling ENgine (FLUMEN). The results revealed that an integrated flood analysis considering the effects of inundation flooding, river flooding, and coastal flooding required evaluation of the risk of flooding in coastal cities.

Keywords: storm surge; river inundation; inland submergence; HDM-2D; coastal cities; integrated flood analysis

1. Introduction

1.1. Backgrounds

Climate change has recently affected the frequency of subtropical rainfall and extreme typhoons, causing flood damage, especially in coastal and riverside areas. The inundation occurring in these areas can be classified as storm surges caused by typhoons or earthquakes, river inundation caused by rising stream water surface elevation because of subtropical rainfall, and the inland submergence caused by rural storm sewer drainage failures.

In coastal urban areas, these various types of flooding occur in a singular or a complex form, causing extensive damage. Therefore, each local government pays attention to disaster prevention strategies by establishing structural and nonstructural measures to reduce flood damage. Structural measures include the construction of L.I.D. (Low Impact Development) systems, reservoirs, urban floodplains, and underground reservoirs. Nonstructural measures encompass improved operation of disaster prevention systems, flood insurance plan, and flood risk mapping. Because the structural measures require constructions of large-scale facilities, they result in budget burdens and environmental problems. Therefore, recent studies have focused on developing inundation risk maps through two-dimensional flow analysis models as nonstructural countermeasures and identifying inundation risks in advance to enable effective disaster prevention budgeting.

1.2. Overview of Current Researches

In the case of two-dimensional flow analysis simulations, the United States Army Corps of Engineers conducted simulations of flood analysis in conjunction with HEC-2 and GRASS models [1]. Fan et al. analyzed the occurrence of flooding in urban areas by linking a 1D sewage model with a 2D flow analysis model [2]. Horritt et al. analyzed 1D flood inundation using the HEC-RAS model developed by the United States Army Corps of Engineers and applied the two-dimensional finite element model 'TELEMAC-2D' and the raster-based 'LISFLOOD-FP' model to simulations of river flooding [3]. Paz et al. illustrated the initial efforts of developing a modeling system configured by connecting a 1D flow routing model to a 2D-raster based model to simulate urban flooding [4]. Adeogun et al. developed a 1D-2D hydrodynamic inundation model by connecting a previously used 1D sewer network model (SWMM) with a 2D flow analysis model [5,6]. This model was used for small urban flooding to determine the appearance of domestic flooding occurring on land. Leandro and Martins linked a 2D river flow model to the Sewage Model SWMM5 to simulate interaction between sewers and overland flow [7]. Moreover, combined 1D-2D models for urban flooding have been developed and applied [8,9]. Substantial efforts have been made to evaluate flood inundation by hydrological models: the estimation of flood frequency by a continuous simulation approach for a dam site was conducted in a large catchment [10]; a distributed rainfall-runoff model was developed to approximate the horizontal flow at a point by means of a kinematic wave model [11]; an analytical distribution formulation of the peak flood and maximum annual peak flood was presented based on a simplified description of rainfall and surface runoff processes [12]; the main mechanisms of runoff generation controlling the flood frequency distribution was identified by regional analysis [13]; and targeting on a significant number of river basins belonging to a humid region, an analytical work based on a stochastic differential equation for the description of the soil water balance and runoff production, was adopted [14].

1.3. Objectives

Previous studies based on the two-dimensional flow analysis modeling have mainly focused on single flood inundation simulations, and existing studies [15,16] usually apply a linear sum of individual inundation components to predict comprehensive flood phenomena. However, this approach does not consider the weighted effects generated by complex flooding that occur at the same time and cause high errors. Therefore, in the present study, a two-dimensional hydrodynamic numerical model for complex flood modeling was developed and quantitative analysis of flooded areas and flow velocity was conducted. The results were then compared with single type flooding simulations.

2. Methods

2.1. Applied Models

To conduct the single and comprehensive inundation simulations, a two-dimensional hydrodynamic model, HDM-2D, was developed, and simulation results generated by this model were compared and analyzed using the commercial two-dimensional flow model FLUval Modeling ENgine (FLUMEN). The two models used in this study are explained below.

HDM-2D is a two-dimensional flow analysis model that discretizes the shallow water equation using the Petrov–Galerkin stabilized scheme for numerical calculation. HDM-2D was first developed for a flow analysis, after which further studies were conducted to develop additional objectives and functions along with verifications of its applicability. The flow model features the following: stability assessment of riverfront facilities on inundated floodplains based on flow characteristics [17]; consideration of nonhydrostatic pressure distributions based on the total acceleration method [18]; prediction of river inundation or discontinuous shock flow by the SU/PG scheme [19]; interlayer connection analysis in underground spaces [20]; and inclusion of an external

flow source by the adaptive transfer method [21]. The preprocessing tools in the RAMS suite package created input conditions for geometrical mesh creation and initial/boundary conditions, while the postprocessing tools displayed the results of the flow velocity and water depth calculations [22]. The HDM-2D is a general purpose two-dimensional surface flow model that can simulate channel flows and urban inundation as described in Figure 1. In this study, the inundation analysis model was used to analyze and numerically predict complex flood situations with multiple sources of inundation, such as storm surges, river inundation, and inland submergence.

	Channel analysis mode	Inundation analysis mode	In-depth analysis mode
			
Time control	<ul style="list-style-type: none"> · Steady · Quasi-unsteady · Unsteady 	<ul style="list-style-type: none"> · Unsteady 	<ul style="list-style-type: none"> · Steady · Quasi-unsteady · Unsteady
Options	<ul style="list-style-type: none"> · Wet and dry process · Hot Start initiation · Suppression of depth wiggling 	<ul style="list-style-type: none"> · Adjustment of time discretization · Sink/source formation · Numerical scheme (Galerkin, SU/PG) 	<ul style="list-style-type: none"> · Turbulence modeling (Constant, Parabolic, Smagorinsky)
Main features	<ul style="list-style-type: none"> · Spatial allocation of inflow discharge profile · Any combination of flow and stage boundary conditions · Transcritical & supercritical flow 	<ul style="list-style-type: none"> · River inundation · Inland flooding 	<ul style="list-style-type: none"> · Secondary current effect via dispersion stress method · Navier-slip boundary condition · Dam break flow · Computation of non-hydrostatic flow

Figure 1. Specifications of the HDM-2D model.

The FLUMEN (FLUvial Modeling ENgine) model was developed by Beffa of Switzerland, and is now being used as an inundation analysis model in countries such as Switzerland, Germany and Austria. The FLUMEN model is a two-dimensional model that uses a depth-averaged shallow water equation with unstructured grids and is proficient in modeling hydraulically complex areas such as river meanders and confluence areas. This model is capable of using wet/dry techniques when modeling various types of topography, and can use both subcritical and supercritical flow modeling. The governing equations, numerical methods, main functions and applications are shown clearly in the FLUMEN manual [23] and in a study conducted by Bae et al. [24].

2.2. Verification of Models

This HDM-2D model was tested against a hydraulic flume problem to check the performance of inundation analysis. Comparisons with the results of hydraulic experiment conducted by Smith et al. [25] were made to verify the model. Additionally, the results were compared with the commercial model FLUMEN. Smith et al. considered a major flood accident that occurred in 2007 in the New Castle Merewether area of Australia to create a downscaled topographic model of 12.5 m in length and 5 m in width to reproduce the flood and analyze the flow characteristics in the experiment (see Figure 2). Smith et al. opened the raw data from the measured observations, and present study used the data set for model verification and comparison.

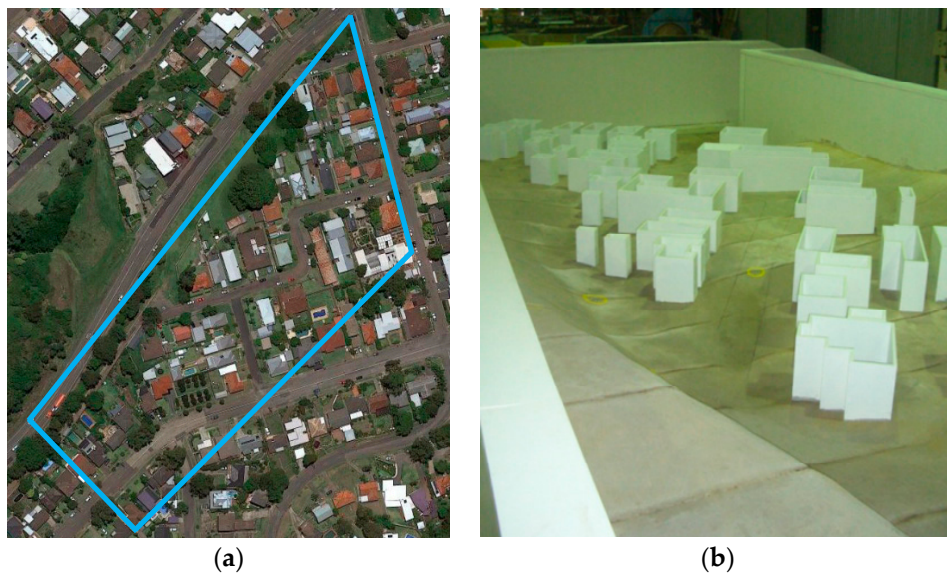


Figure 2. Verification domain for checking model performance of inundation analysis. (a) Flooded areas in New Castle, Australia. (b) Scaled reproduction by hydraulic flume.

The HDM-2D model was capable of reaching a converged result using steady state simulation mode, but the FLUMEN model did not have a steady state simulation function; therefore, unsteady simulation was executed for a long-term period until the input and output flow discharge were equal and the velocity did not change. This study used the same values of boundary conditions and parameters used by Smith et al. The input flow discharge was $19.7 \text{ m}^3/\text{s}$ and the left and right boundaries were assigned as transmissivity conditions. The manning coefficient that would affect the runoff flow was determined to be 0.020. As shown in Figure 3, 13 points were selected as comparison locations because the effects of the buildings interfering with the runoff flow were evident as water flowed quickly through the roads located in the lowland region.

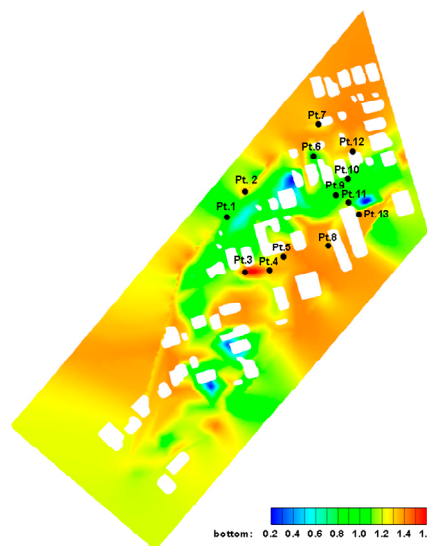


Figure 3. Comparison points for verification of models.

2.3. Model Selection

Table 1 shows the results of the velocity and depth in the selected area. In cases of the inundation depth, the average discrepancy between the HDM-2D model results and the experimental values was found to be 0.08 m, while for the FLUMEN model, this value was 0.11 m, indicating that the HDM-2D model had an accuracy 26% better than the FLUMEN model.

Table 1. Depth and velocity comparisons between measured and predicted results.

# of Point	Measured Depth [25] (m)	HDM-2D Depth (m)	FLUMEN Depth (m)	Measured Velocity [25] (m/s)	HDM-2D Velocity (m/s)	FLUMEN Velocity (m/s)
1	0.721	0.660	0.658	0.9	0.901	0.402
2	0.442	0.412	0.369	0.9	1.098	0.671
3	0.1	0.100	0.101	0.6	0.673	0.492
4	0.406	0.348	0.342	0.8	0.703	0.525
5	0.442	0.379	0.359	0.6	0.555	0.382
6	0.784	0.631	0.615	0.9	0.644	0.432
7	0.523	0.466	0.384	0.7	0.764	0.373
8	0.442	0.363	0.337	0.8	0.707	0.411
9	0.766	0.629	0.614	1.0	0.913	0.776
10	0.712	0.567	0.553	0.6	0.711	0.717
11	0.604	0.469	0.422	1.3	1.128	1.059
12	0.397	0.269	0.247	0.7	0.707	0.763
13	0.388	0.360	0.280	0.6	0.380	0.146

Figure 4a,b shows the inundation modeling results for a contour type, and Figure 4c is a graph showing the inundation depth results. Both models showed similar characteristics with comparable depth distributions in the inflow area, outflow region, and left/right boundaries. However, the HDM-2D model showed better performance in the roads of the lowland areas and the front/sides of buildings, where the inundation depth was higher than for other areas. Therefore, the HDM-2D model more accurately predicted inundation depth than the FLUMEN.

Prediction of the flow velocity by the HDM-2D model and FLUMEN led to considerable differences as shown in Figure 5. When compared with the experimental results, the HDM-2D prediction had an average discrepancy of 0.11 m/s. In contrast, the FLUMEN model had a mean difference of 0.28 m/s, and its error is 61% higher than the HDM-2D model results. The difference between the results of the two models became noticeable near the areas of densely concentrated building structures. These findings indicated that the HDM-2D model is better at recognizing buildings as internal boundaries because it uses generalized boundary fitting coordinates.

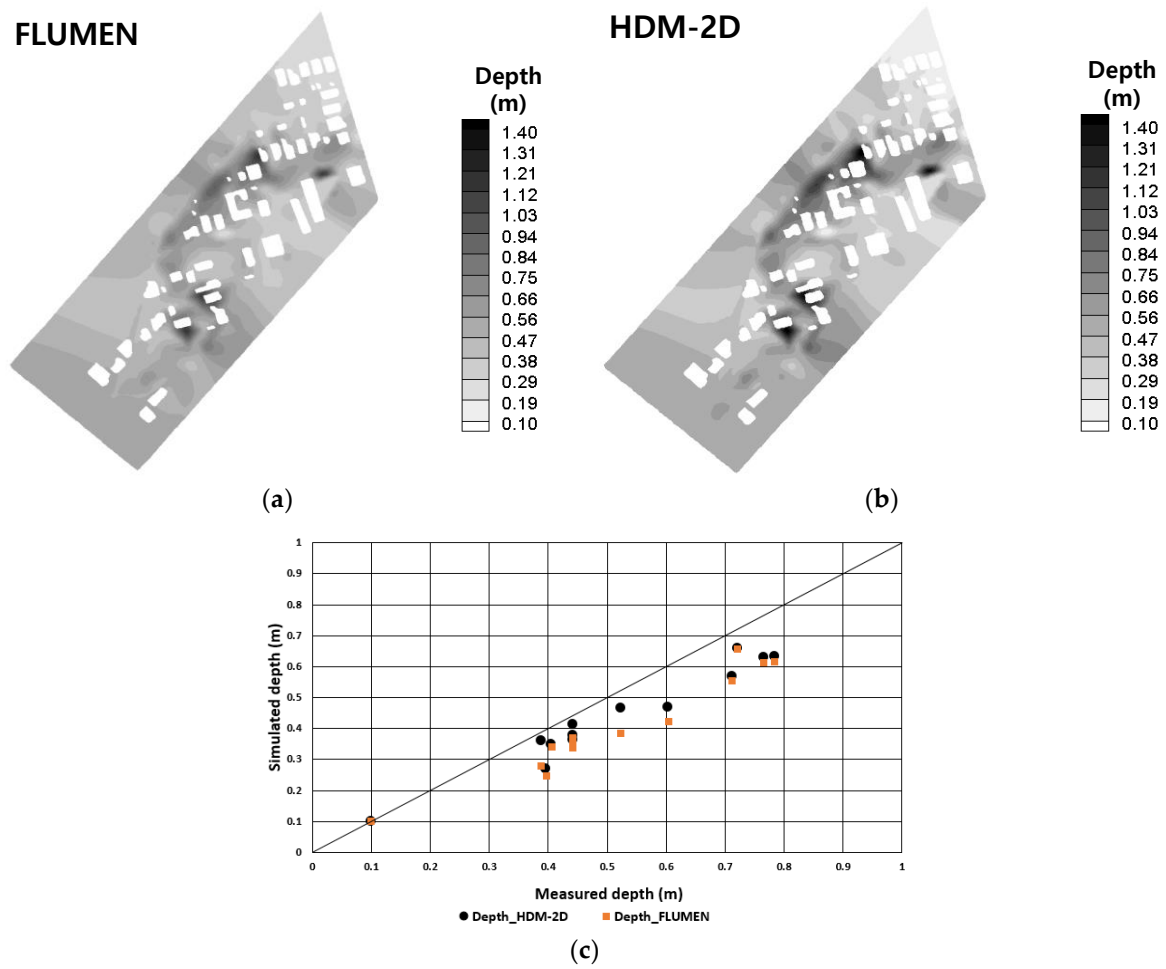


Figure 4. Comparison of inundation depth. (a) Depth contour by FLUval Modeling Engine (FLUMEN) model; (b) depth contour by HDM-2D model; and (c) scatter plot.

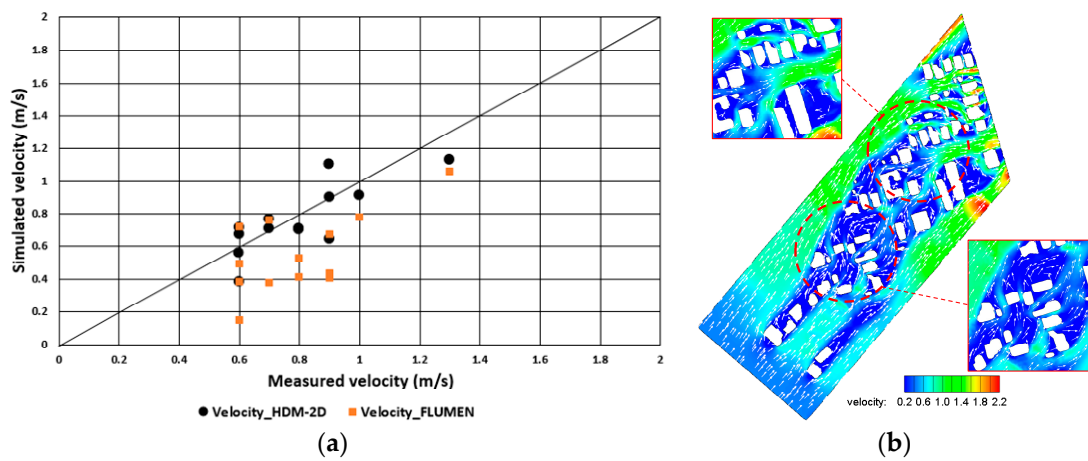


Figure 5. Comparison of flow velocity. (a) Scatter plot and (b) velocity contour by HDM-2D model.

3. Results

3.1. Study Area

The Masan free trade zone is a national industrial zone in South Korea that suffered immense damage from Typhoon Maemi in September of 2003. The local area is adjacent to the ocean in the south and near the Sanho River, which makes it vulnerable to storm surges and river inundation. Additionally, the area was artificially developed by land reclamation; therefore, drainage is problematic, which causes frequent inland submergence. Because of these conditions, the area is susceptible to comprehensive flooding. Accordingly, this study used the HDM-2D model for single and comprehensive flood simulations and compared the modeling results quantitatively with or without using the effects of multisource flooding.

3.2. Topography Reproduction

The selected target area consisted of 0.21 km² within the Masan free trade zone encompassing the ocean in the south and the Sanho River in the west. This study used a numerical digital map and DEM data from the National Geographic Information Institute to produce the topography for the two-dimensional flow analysis. As shown in Figure 6, the mesh layout consisted of 36,669 nodes and 42,300 elements. In addition, every building within the target area was included in the computational domain because they could disturb the runoff flow.

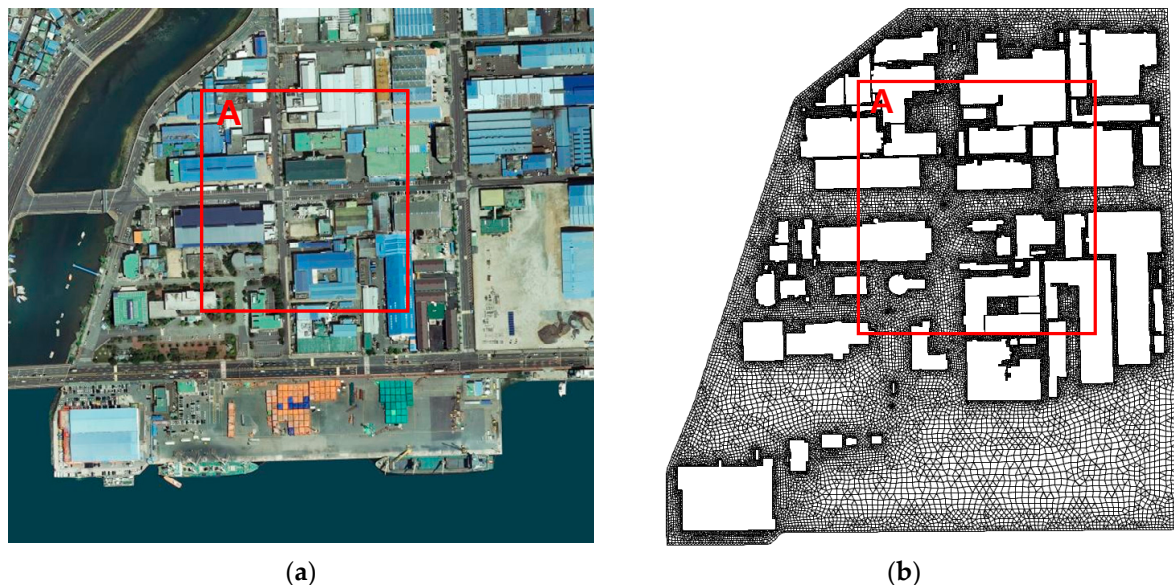


Figure 6. Terrain of inundation analysis area. (a) Plan view of Masan free trade zone. (b) Mesh layout. (*A is the domain used in Figure 9).

3.3. Simulation Setups

The basic background and boundary conditions for the simulations are described below. As suggested by Kawai et al. [26], the Masan free trade zone had a mean tidal level of 1.5 m, but Typhoon Maemi on September 12, 2003 caused an increase of tidal level up to 4.5 m at its peak (see Figure 7a). As a result, seawater overflowed into the Masan free trade zone, and the maximum inundation height by storm surge reached 3.0 m during this event. As pointed out by Kawai et al. [26], obvious inundation evidences remained on the wall around the wharf building, and the traces demonstrated this guess. Moreover, as presented in Figure 7b, the total precipitation from September 11th to 13th was 178.0 mm. During this period, heavy rainfall from upstream accumulated and combined with a large amount of water that failed to drain, aggravating the flood damage. River inundation is usually caused by extreme rainfall, but this area faces the estuary near

the ocean, and flooding during this event was primarily caused by sea water overflow. Therefore, the river inundation depth was set to be the same as for the storm surge condition (3 m). The inland submergence effects were also considered, so the typical runoff caused by a 30 cm diameter manhole was applied to the flood simulation.

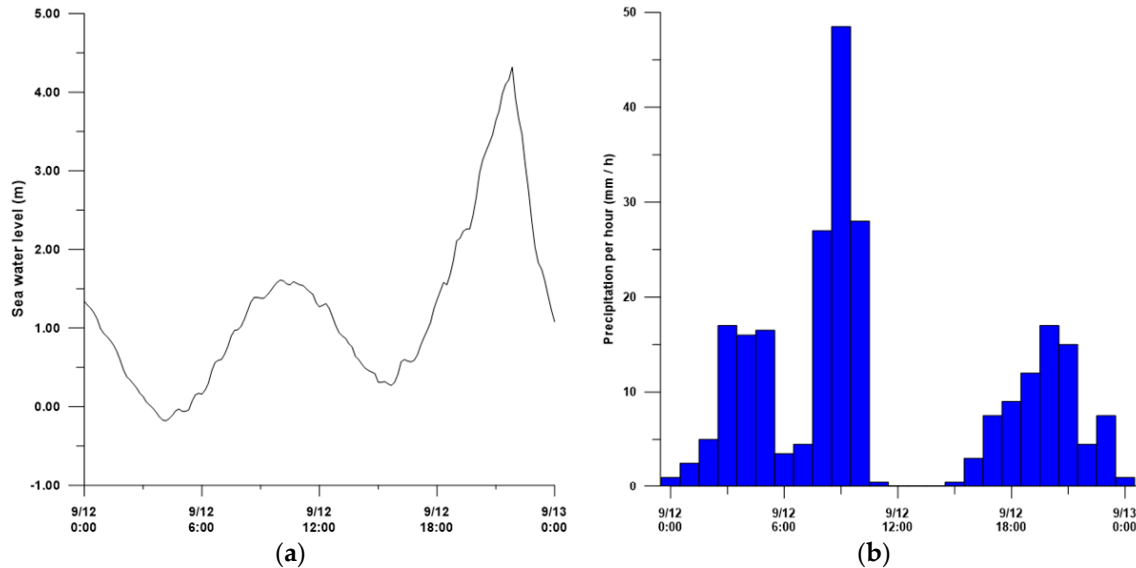


Figure 7. Trigger for comprehensive inundation. (a) Abrupt increase in tidal elevation. (b) Rainfall hyetograph by downpour.

3.4. Single and Comprehensive Inundation Modeling

In this study, the single flood simulation refers to the numerical modeling of the flood phenomena considering only one submerging source among the inland flooding, river inundation, and storm surge, while the comprehensive flood simulation means the flood prediction by combination of multiple sources. The five simulation cases for single (Cases 1, 2, and 3) and comprehensive (Cases 4 and 5) simulations are shown in Table 2.

Table 2. Simulation cases for single source (Cases 1, 2, and 3) and multiple source (Cases 4 and 5) inundation.

Classification	Conditions	Case 1	Case 2	Case 3	Case 4	Case 5
Inland flooding	0.14 m ³ /s	o	-	-	-	o
River inundation	3 m	-	o	-	o	o
Storm surge	3 m	-	-	o	o	o

4. Discussions

It needs to be mentioned that the modeling performance should be evaluated with observed data. However, the Typhoon Maemi in 2003 triggered the most severe coastal disaster in Korea [26], and the Masan Bay had unprecedented damage by landing of the extreme storm surge. The tidal observation tower was destroyed due to the high wave. Therefore, the quantitative comparison with observed data was very hard to conduct. Instead, obvious inundation evidences remained on the wall around the wharf building, and the traces comply with the modeling results. Accordingly, this section is dedicated to the comparison of the single flooding with the comprehensive flooding simulation.

The following comparisons between single flood type simulations and comprehensive flood simulations were made. Because the most severe flooding occurred at the Case 5 and almost the entire simulation domain was submerged after 400 s from the inundation beginning (see Table 3 and

Figure 8), the flood properties were analyzed at $t = 400$ s. For Case 1, the flood damage was simulated to be the lowest of the results with 17.1% of the area flooded; while Case 2 and Case 3 were 34.9% and 60.8% of the area flooded, respectively, at 400 s after inundation began (see Figure 8). However, for the comprehensive flow simulations in Cases 4 and Case 5, 84% and 91.7% of the area were flooded, respectively. When the linear sum of an individual inundation component was adopted, the error was over 20% when compared with the comprehensive flood. Moreover, the inundation depth was higher in the comprehensive flood simulation while the flow velocity at 400 s was 0.38 m/s and 0.43 m/s for Cases 2 and 3, respectively, but Cases 4 and 5 showed lower values of 0.35 m/s and 0.33 m/s, respectively. This is because the flows from different sources merged, and each flow decreased in velocity with stagnation. Table 3 lists the comparison result.

Table 3. Comparison of flood properties.

Attributes	Unit	Case 1	Case 2	Case 3	Case 4	Case 5
Flooded area	%	17.1	34.9	60.8	84	91.7
Maximum flooding depth	m	1.36	1.94	1.99	2.08	2.08
Average flooding depth	m	0.173	0.35	0.43	0.47	0.48
Maximum flooding velocity	m/s	2.71	2.84	2.75	2.76	2.76
Average flooding velocity	m/s	0.32	0.38	0.43	0.35	0.33

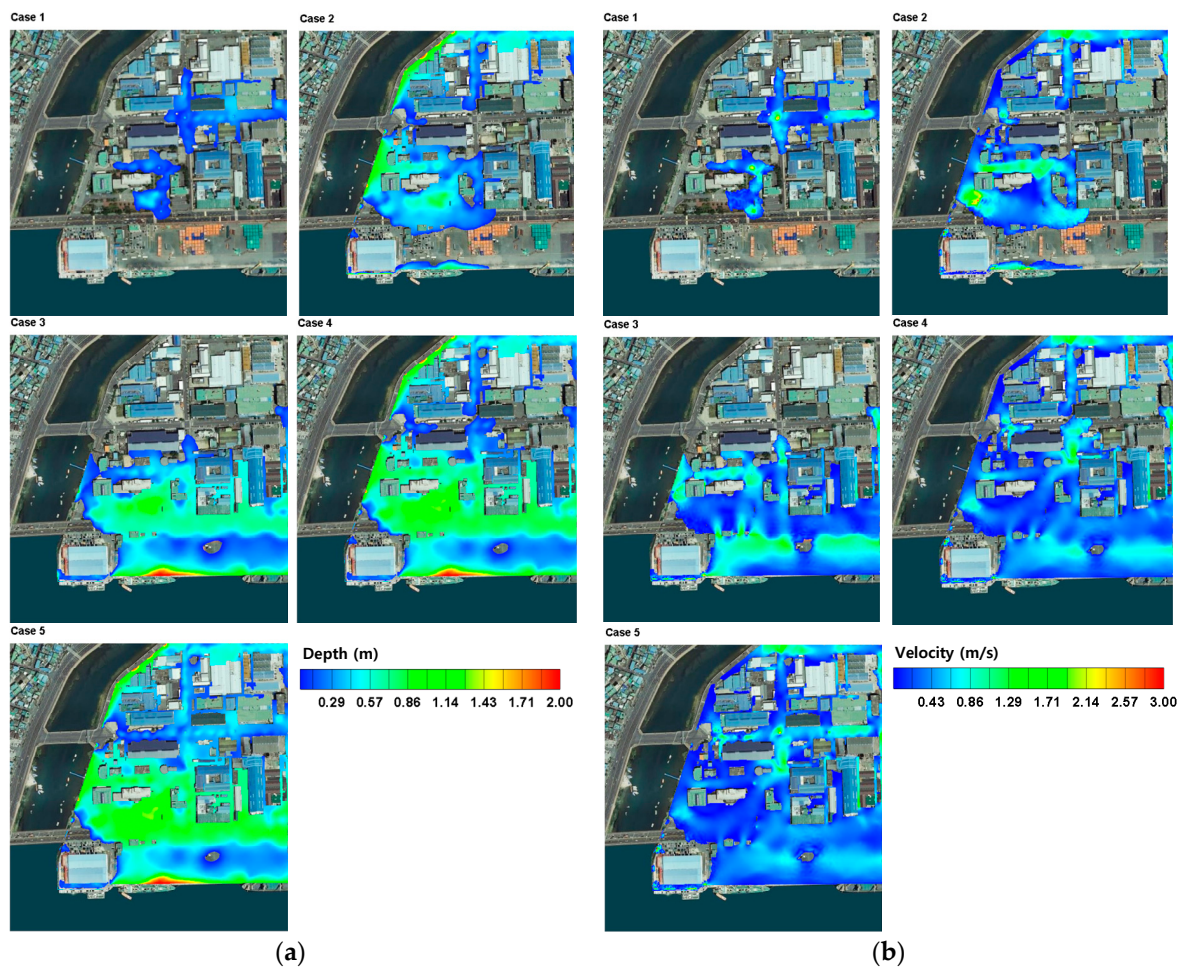


Figure 8. Spatial variations of flooding according to inundation source(s) at $t = 400$ s. (a) Depth. (b) Velocity.

Targeting on the region marked 'A' in Figure 6, the inundation depth and flow velocity were investigated along the four checking lines of Figure 9. Similar to the Figure 8, Figure 9 was plotted at $t = 400$ s. As shown in Figure 9, the inundation depth increased from 22.7% to 52.7% along the four lines in Case 5 and the flow velocity increased from 21.1% to 81.7%. In addition, the linear sum of single simulations in a small area does not reflect the momentum effect of encountering different types of flood waves, and thus shows great differences when compared with the complex simulations that can reflect this. These results demonstrated the significance of conducting multi source flood modeling to show the effects of changes in flow velocity and inundation depth when comprehensive flooding occurs in areas of confluence or divergence.

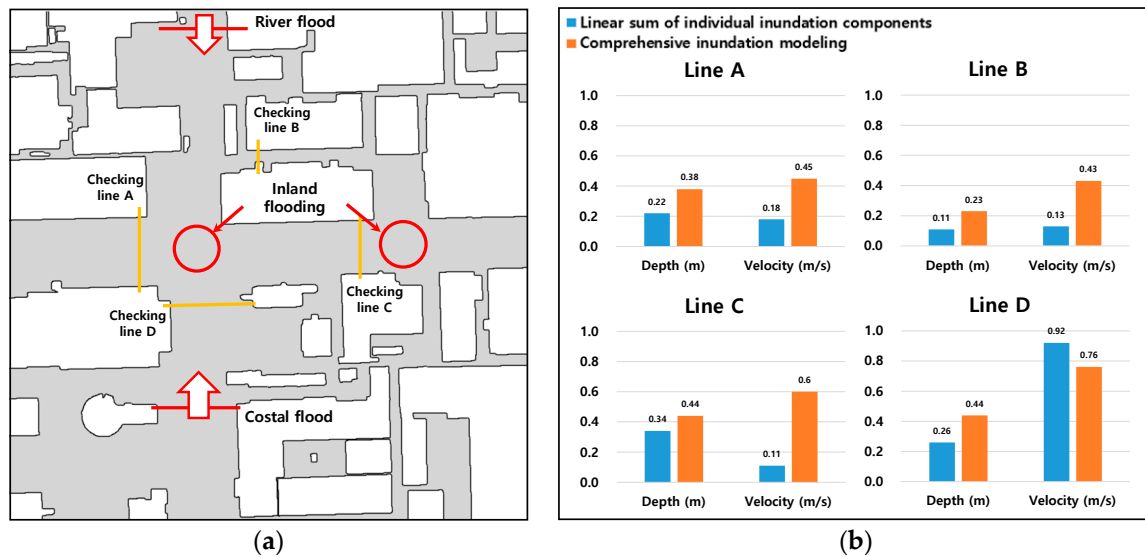


Figure 9. Comparison of inundation depth and flow velocity along the checking lines ($t = 400$ s) (a) Locations of checking line. (b) Comparison between individual sum and comprehensive modeling along checking lines.

In summary, the difference in flooded areas between the summation of inundated space identified by the single source flooding simulations and the submerged region identified by multisource flood simulations was as high as 20%. Therefore, these results show that the former method of using a linear sum of individual inundation components can cause higher error in the calculation results. For areas with frequent occurrences of comprehensive flooding such as estuaries, nearby rivers or coastal cities, various sources of the flooding must be considered together and comprehensive flood simulation is necessary.

5. Summary and Conclusions

In coastal urban areas, various types of flooding occur in a singular or a complex form, causing extensive damage. However, previous studies [15,16] usually applied a linear sum of individual inundation components to predict comprehensive flood phenomena; this approach does not consider weighted effects associated with the simultaneous occurrence of flooding with multiple sources. Therefore, in this study, a two-dimensional hydrodynamic numerical model for complex flood analysis was developed and verified against an urban inundation problem. The experimental measurements that reproduced a flood in New Castle, Australia in 2007 were utilized. The developed model provided accurate results in predicting inundation flow behavior, and as for inundation depth, the developed model performed 26% better than a commercial model.

In this study, the single flood simulation refers to the numerical modeling of the flood phenomena considering only one submerging source among the inland flooding, river inundation, and storm surge, while the comprehensive flood simulation means the flood prediction by combination of multiple

sources. When water that overflowed from the sea and the river converged with inland water in the comprehensive flooding simulation, the inundation depth increased from 20.4% to 63.6% and the flow velocity increased from 10.5% to 81.7% compared with the single flood simulation. The difference in flooded areas between the summation of inundated space identified by the single source flooding simulations and the submerged region identified by multisource flood simulations was as high as 20%. The single flood modeling or a linear sum of individual inundation components fails to capture the dynamic nature of inundation appropriately and can underestimate the flooding damage, which can cause higher error in the calculation results.

For areas with frequent occurrences of comprehensive flooding such as estuaries, nearby rivers or coastal cities, various sources of the flooding must be considered simultaneously. The comprehensive inundation modeling approach can provide useful tools for coastal designing, predictive measures for flooding, and improvements of preparedness in evacuations. Thereby, coastal societies can better estimate their flood disaster risks. Further studies are now being prepared to extend the area of application domain by adaptive mesh reformulation strategy. In addition, the model performance on the computational speed must be improved for the practical purpose.

Author Contributions: Conceptualization, C.G.S. and D.S.R.; Formal Analysis, E.T.S.; Data Curation, E.T.S. and J.S.; Supervision, C.G.S.; Writing—Original Draft, E.T.S.; Writing—Review & Editing, J.S., D.S.R., H.-J.K., and C.G.S.

Acknowledgments: This work was funded by an Incheon National University Research Grant in 2018.

Conflicts of Interest: The authors declare no conflicts of interest.

References

1. Davis, C.A. *Floodplain Analysis Tools, User's Documentation*; US Army Corps of Engineers, Hydrologic Engineering Center: Second Street Davis, CA, USA, 1992.
2. Fan, Y.; Ao, T.; Yu, H.; Huang, G.; Li, X. A Coupled 1D–2D Hydrodynamic Model for Urban Flood Inundation. *Adv. Meteorol.* **2017**, *2017*, 2819308. [[CrossRef](#)]
3. Horritt, M.S.; Bates, P.D. Evaluation of 1D and 2D numerical models for predicting river flood inundation. *J. Hydrol.* **2002**, *326*, 87–99. [[CrossRef](#)]
4. Paz, A.R.; Meller, A.; Silva, G.B.L. Coupled 1D-2D hydraulic simulation of urban drainage system: Model development and preliminary results. In Proceedings of the 12th International Conference on Urban Drainage, Porto Alegre, Brazil, 11–16 September 2011.
5. Adeogun, A.G.; Pathirana, A.; Daramola, M.O. 1D-2D hydrodynamic model coupling for inundation analysis of sewer overflow. *J. Eng. Appl. Sci.* **2012**, *7*, 356–362. [[CrossRef](#)]
6. Adeogun, A.G.; Daramola, M.O.; Pathirana, A. Coupled 1D-2D hydrodynamic inundation model for sewer over-flow. *Water Sci.* **2015**, *29*, 146–155. [[CrossRef](#)]
7. Leandro, J.; Martins, R. A methodology for linking 2D overland flow models with the sewer network model SWMM 5.1 based on dynamic link libraries. *Water Sci. Technol.* **2016**, *73*, 3017–3026. [[CrossRef](#)] [[PubMed](#)]
8. Leandro, J.; Chen, A.S.; Djordjevic, S.; Savic, D.A. Comparison of 1D/1D and 1D/2D Coupled (Sewer/Surface) Hydraulic Models for Urban Flood Simulation. *J. Hydraul. Eng.* **2009**, *135*, 495–504. [[CrossRef](#)]
9. Seyoum, S.D.; Vojinovic, Z.; Price, R.K.; Weesakul, S. Coupled 1D and Noninertia 2D Flood Inundation Model for Simulation of Urban Flooding. *ASCE J. Hydraul. Eng.* **2012**, *138*, 23–34. [[CrossRef](#)]
10. Blazkova, S.; Beven, K. Flood frequency estimation by continuous simulation of subcatchment rainfalls and discharges with the aim of improving dam safety assessment in a large basin in the Czech Republic. *J. Hydrol.* **2004**, *292*, 153–172. [[CrossRef](#)]
11. Ciarapica, L.; Todini, E. TOPKAPI: A model for the representation of the rainfall-runoff process at different scales. *Hydrol. Proc.* **2002**, *16*, 207–229. [[CrossRef](#)]
12. De Michele, C.; Salvadori, G. On the derived flood frequency distribution: Analytical formulation and the influence of antecedent soil moisture condition. *J. Hydrol.* **2002**, *262*, 245–258. [[CrossRef](#)]
13. Fiorentino, M.; Gioia, A.; Iacobellis, V.; Manfreda, S. Regional analysis of runoff thresholds behaviour in Southern Italy based on theoretically derived distributions. *Adv. Geosci.* **2011**, *26*, 139–144. [[CrossRef](#)]

14. Gioia, A.; Manfreda, S.; Iacobellis, V.; Fiorentino, M. Performance of a theoretical model for the description of water balance and runoff dynamics in southern Italy. *J. Hydrol. Eng.* **2014**, *19*, 1113–1123. [[CrossRef](#)]
15. Ray, T.; Stepinski, E.; Sebastian, A.; Bedient, P.B. Dynamic modeling of storm surge and inland flooding in a Texas coastal floodplain. *J. Hydraul. Eng.* **2011**, *137*, 1103–1110. [[CrossRef](#)]
16. Chen, W.B.; Liu, W.C. Modeling flood inundation induced by river flow and storm surges over a river basin. *Water* **2014**, *6*, 3182–3199. [[CrossRef](#)]
17. Song, C.G.; Ku, Y.H.; Kim, Y.D.; Park, Y.S. Stability analysis of riverfront facility on inundated floodplain based on flow characteristic. *J. Flood Risk Manag.* **2018**, *11*, 455–467. [[CrossRef](#)]
18. Rhee, D.S.; Lyn, S.W.; Song, C.G. Numerical Computation of Rapid Flow over Steep Terrain Using Total Acceleration Method. *J. Coast. Res.* **2018**, *85*, 986–990. [[CrossRef](#)]
19. Song, C.G.; Oh, T.K. Transient SU/PG modelling of dis-continuous wave propagation. *Prog. Comput. Fluid Dyn.* **2016**, *16*, 146–162. [[CrossRef](#)]
20. Kim, H.J.; Rhee, D.S.; Song, C.G. Numerical Computation of Underground Inundation in Multiple Layers Using the Adaptive Transfer Method. *Water* **2018**, *10*, 85. [[CrossRef](#)]
21. Kim, S.E.; Lee, S.E.; Kim, D.W.; Song, C.G. Stormwater Inundation Analysis in Small and Medium Cities for the Climate Change Using EPA-SWMM and HDM-2D. *J. Coast. Res.* **2018**, *85*, 991–995. [[CrossRef](#)]
22. Park, I.H.; Seo, I.W.; Kim, Y.D.; Song, C.G. Flow and dispersion analysis of shallow water problems with Froude number variation. *Environ. Earth Sci.* **2016**, *75*, 120. [[CrossRef](#)]
23. FLUMEN User Manual. Available online: <https://www.fluvial.ch/manual.html> (accessed on 2 February 2019).
24. Bae, Y.H.; Koh, D.K.; Cho, Y.S. Numerical simulations of flood inundations with FLUMEN. *J. Korea Water Resour. Assoc.* **2005**, *14*, 355–364. (In Korean) [[CrossRef](#)]
25. Smith, G.P.; Wasko, C.D.; Miller, B.M. *Modelling the Influence of Buildings on Flood Flow*; Water Research Laboratory, University of New South Wales: Sydney, NSW, Australia, 2012.
26. Kawai, H.; Kin, D.S.; Kang, Y.k.; Tomita, T.; Hiraishi, T. Hindcasting of Storm Surge at Southeast Coast by Typhoon Maemi. *J. Ocean Eng. Technol.* **2005**, *19*, 12–18.



© 2019 by the authors. Licensee MDPI, Basel, Switzerland. This article is an open access article distributed under the terms and conditions of the Creative Commons Attribution (CC BY) license (<http://creativecommons.org/licenses/by/4.0/>).